MODELS FOR SAFETY ANALYSIS OF THE GENERATION IV SUPERCRITICAL WATER-COOLED REACTOR

G. Harrisson[1] and G. Marleau[1]
[1]Institut de génie nucléaire, École Polytechnique de Montréal, Québec, Canada

Abstract

The nuclear performance analysis of the pressure tube version of the Supercritical Water-Cooled Reactor (SCWR) requires the study of the neutron population in its lattice cell. Studies involving assemblies of SCWR cells are also needed to take into account environmental effects. In this paper, we present the SCWR lattice cell model that has been developed using the DRAGON code. The radial and Cartesian mesh discretization as well as the tracking parameters have been optimized based on the study of the multiplication constant and two groups cell averaged cross sections.

The assembly model we selected corresponds to a checkerboard pattern with two different cell types (different local properties such as coolant and fuel temperature) and periodic boundary conditions. Comparisons of the multiplication constant, neutron spectra and reaction rates obtained from the cell and assembly models indicate that a strong coupling exists between neighboring cells because the light water coolant has a significant effect on neutron slowing-down and neutron absorption.

1. Introduction

The Supercritical Water-Cooled Reactor (SCWR) is one of the six nuclear systems selected by the Generation IV International Forum [1]. Both pressure vessel and pressure tube versions of the SCWR are designed to operate with temperatures and pressures above the thermodynamic critical point of water (374°C and 22.1 MPa). The pressure tube version of the SCWR considered in this paper is a natural evolution of the CANDU reactors. Its reference design has an operating pressure of 25 MPa, a reactor inlet temperature of 350°C and a reactor outlet temperature of 625°C [2].

As presented in this paper, the thermodynamic properties found in the SCWR, such as the coolant density, influence significantly the neutron spectrum. The fission power distribution in the reactor, which depends on this neutron spectrum, in turn, influences the thermodynamic properties of the reactor. Thus, safety analysis based on coupled neutronic/thermal–hydraulic studies must be realized in order to ensure the excellence in safety and reliability and to ensure a very low likelihood and a very low degree of reactor core damage under postulated accident scenario [3]. The SCWR is a nuclear system and the neutron population in the reactor core dictates its behavior. Thus, prior to realize coupled studies, it is important to understand the neutronic behavior of the reactor core. In reactor physics, neutronic studies imply a calculation procedure that is divided into two steps. First, a multigroup lattice cell calculation based on the neutron transport equation must be realized in 2-D or in 3-D in order to take into account the interaction of the neutrons with the materials of the lattice cell. Then, a fewgroup finite reactor calculation based on the diffusion equation must be performed in 3-D, using the database generated by the lattice cell calculation, in order to take into account of the whole reactor core. The deterministic codes

DRAGON [4] and DONJON [5], respectively for lattice cell and reactor calculations, are used to demonstrate the nuclear performances of the SCWR.

Here, we will consider the first step in this nuclear safety analysis, namely to study the neutron population in the SCWR lattice. In section 2, we present the development of the SCWR lattice cell model in DRAGON. We then discuss in details the SCWR geometry, the spatial mesh discretization optimization of this geometry and the tracking parameters optimization. Because the lattice pitch of the SCWR is relatively small (between 20 cm and 21 cm [2]) and the thermodynamic conditions of the SCWR vary widely from the reactor inlet to the reactor outlet, it is necessary to study the interaction between adjacent lattice cells from an assembly of lattice cells. In section 3, we present the construction and the verification of a 2x2 assembly of SCWR lattice cells. Finally, from an assembly in checkerboard pattern with two types of lattice cells, we have evaluated the environmental effects of the light water coolant density in SCWR assemblies.

The models presented in this paper simulate the exact assemblies of the SCWR with the `NXT:` tracking module of DRAGON 3.06. In all cases, the collision probability (CP) method has been used to solve the neutron transport equation. The problems have been solved for the infinite multiplication factor (without neutron leakage) with a fixed buckling. The microscopic cross sections used here come from a library in WIMS-D4 format with an energy discretization into 69 groups.

2. Description of the SCWR lattice cell model

The development of the SCWR lattice cell model has been realized in three steps. First, the SCWR geometry has been defined in DRAGON. Second, the spatial mesh discretization of the geometry has been optimized. It must be sufficient to ensure constant sources and constant flux over spatial regions of the geometry (CP approximation). Third, the tracking parameters have been optimized. The density of the integration lines should be as high as possible to touch as often as possible each region and each surface of the geometry. Similarly, the number of integration angles should be as high as possible because the neutron travels on a straight line in the CP method.

2.1 SCWR geometry

The fuel elements and the fuel channels of the SCWR are still in development. In this study, the SCWR lattice cell is composed of a 43 elements CANFLEX® fuel bundle and of a high efficiency fuel channel (HEC) [6] as shown in Figure 1a.

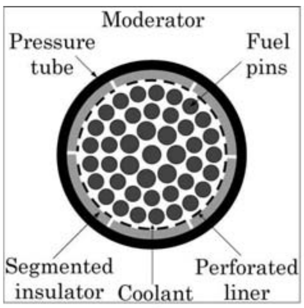

a

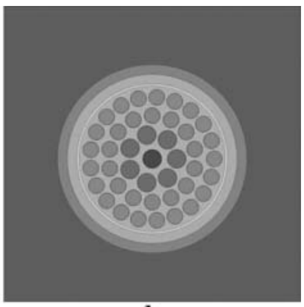
b

Figure 1 SCWR lattice cell (a) SCWR geometry in DRAGON (b)

The four fuel rings of the fuel bundle contain 1, 7, 14 and 21 fuel pins respectively. In this study, all the fuel pins are composed of uranium oxide enriched at 4.25%. The fuel sheath is composed of stainless steel. The light water coolant is brought to supercritical conditions. The fuel bundle is contained in a perforated liner made of stainless steel, in a segmented insulator made of zirconium oxide and in a pressure tube composed of a zirconium alloy (EXCEL). The pressure tube is in direct contact with the heavy water moderator. As shown in Figure 1b, it is not possible to define segmented and perforated regions in DRAGON. Thus, for the SCWR geometry description in DRAGON, the insulator and the liner regions contain, respectively, 70% and 45% of light water (at the coolant pressure and temperature). The lattice pitch has been fixed to 21 cm for this study. Finally, isotropic reflection boundary conditions have been applied uniformly on all the external surfaces of the geometry.

2.2 Spatial mesh discretization optimization

The optimization of the spatial mesh discretization of the geometry has been realized in two steps: (1) the radial mesh optimization followed by (2) the Cartesian mesh optimization.

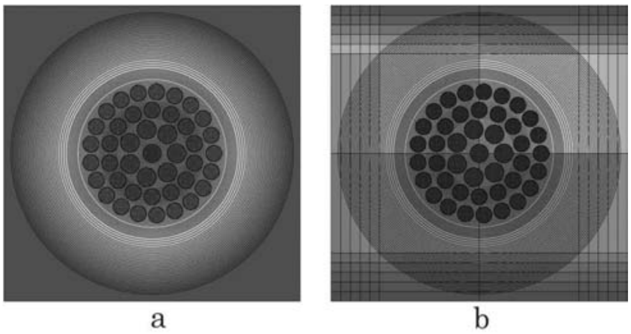

Figure 2 Optimization of the radial (a) and Cartesian (b) mesh discretization

As shown in Figure 2a, the mesh discretization for the moderator region along the radial direction is limited by the boundaries of the geometry in a square lattice cell. Thus, the corners of the geometry are left without mesh discretization. To solve this problem, a mesh discretization along the X-axis and the Y-axis has been added in the moderator region as shown in Figure 2b.

The spatial mesh discretization and the tracking parameters were first optimized by studying the neutronic parameters presented in Table 1. The neutronic parameters have been condensed into two energy groups with the cutoff energy at 0.625 eV and homogenized over the entire cell (group 1 is the fast group and 2 the thermal group).

Table 1 Neutronic parameters used to optimize the SCWR geometry in DRAGON

Neutronic parameters	Description
k_∞	Infinite multiplication constant
$\nu\Sigma_f^1$ and $\nu\Sigma_f^2$	Product of the average number of neutrons produced per fission with the fission cross section for group 1 and 2
Σ^1 and Σ^2	Total cross section for group 1 and 2
$\Sigma_s^{1\to1}$, $\Sigma_s^{1\to2}$, $\Sigma_s^{2\to1}$ and $\Sigma_s^{2\to2}$	Scattering cross section from initial (i) to final (f) group ($i \to f$)

These optimizations have been performed for fresh fuel and for the first and the twelfth fuel bundle in a 594 cm long SCWR fuel channel. Table 2 presents the thermodynamic conditions found in the center of these fuel bundles [7].

Table 2 Thermodynamic conditions used to optimize the SCWR geometry in DRAGON

Fuel bundle	Coolant temperature (°C)	Coolant density (g/cm^3)	Pressure (MPa)
1st	390	0.215	25
12th	615	0.069	25

2.2.1 Radial mesh discretization optimization

The SCWR geometry is divided into 7 regions: fuel, fuel sheath, coolant, liner, insulator, pressure tube and moderator. For each region, the neutronic parameters have been studied as a function of the number of sub-regions *n* in the discretized region (leaving all other regions of the geometry without mesh discretization). The number of sub-regions has been increased by a factor *n* until the neutronic parameters converge. For example, Figure 3 shows the effect on the various neutronic parameters of the radial mesh discretization of the coolant region in the 12th fuel bundle.

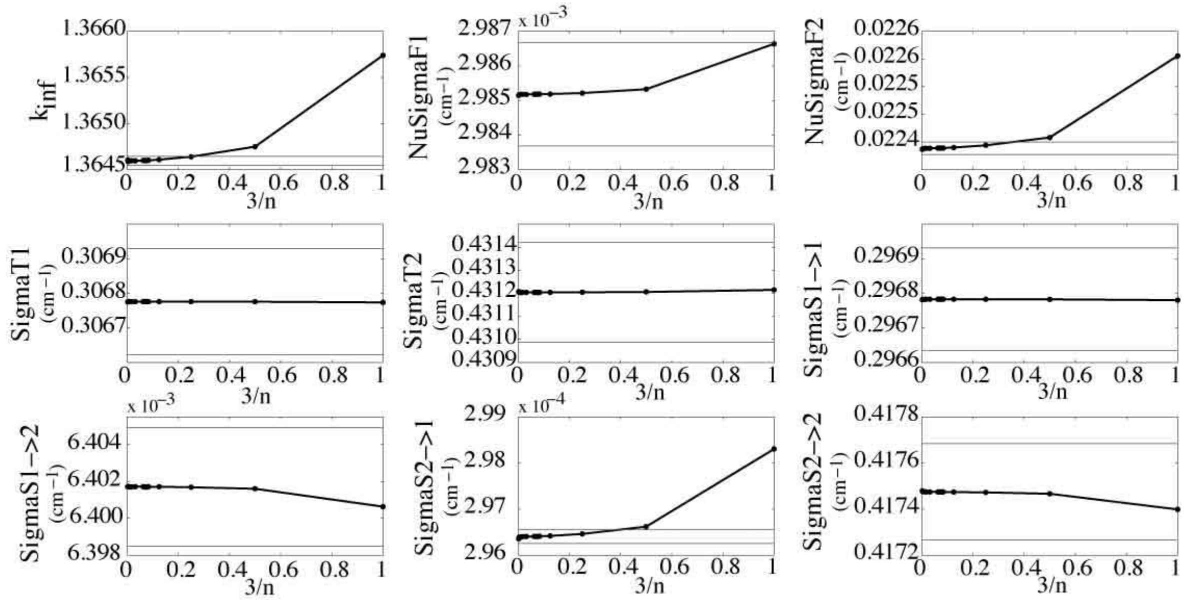

Figure 3 Effect on the neutronic parameters of the radial mesh discretization of the coolant region in the 12th fuel bundle

This study has shown that the convergence of the neutronic parameters is achieved when the fuel pins, the fuel sheaths, the coolant, the liner, the insulator, the pressure tube and the moderator regions are subdivided radially into 32, 1, 193, 8, 32, 32 and 160 sub-regions of equal volumes respectively. This fine mesh discretization produces a geometry with $N = 559$ independent sub-regions for the neutron flux calculation in DRAGON. This number is relatively high considering that (1) a Cartesian mesh discretization must be added to the geometry, (2) this geometry will be used to build a 2x2 assembly with 4 lattice cells and (3) the collision probability method generates full matrices with N^2 elements.

To limit the simulation time and the memory space needed to perform the calculations, the number of sub-regions produced by the radial mesh discretization has been reduced. The following criterions have allowed the selection of the optimized radial mesh discretization:

- A maximum deviation of 0.1 mk centered on the converged value is tolerated for k_∞;
- A maximum deviation of 0.1% centered on the converged value is tolerated for all the macroscopic cross sections.

In Figure 3, the horizontal lines represent these criterions. It shows that k_∞, $\nu\Sigma_f^2$ and $\Sigma_s^{2\to1}$ limit the choice of the radial mesh discretization of the coolant region. In fact, we have observed that these three parameters limit the choice of the radial mesh discretization of all the regions of the geometry.

The optimized radial mesh discretization results in the fuel pins, the fuel sheaths, the coolant, the liner, the insulator, the pressure tube and the moderator regions being subdivided radially into 8, 1, 50, 1, 8, 4 and 25 sub-regions respectively. This optimized radial mesh discretization results in N = 125 independent sub-regions. Figure 2a shows this mesh discretization.

2.2.2 Cartesian mesh discretization optimization

Next, the geometry has been subdivided into four parts. This division has been considered to take into account of environmental effects in assemblies of lattice cells. In principle, the addition of these subdivisions in the geometry should not affect strongly the results of lattice cell calculations. We have observed, from lattice cell calculations performed with the conditions in Table 2, that this is the case (no effect on the k_∞ and a difference of less than 0.0002% on the macroscopic cross sections).

Next, the Cartesian mesh discretization of the geometry has been optimized for the four corners at the same time. The neutronic parameters have been studied as a function of the number of squares present in the corners of the geometry. The number of squares has been increased until the neutronic parameters converge. 256 squares per corner are required to reach this convergence.

The optimization criteria described in section 2.2.1 have allowed the selection of the optimized Cartesian mesh discretization. Again, we have observed that k_∞, $\nu\Sigma_f^2$ and $\Sigma_s^{2\to1}$ limit the choice of the Cartesian mesh discretization of the corners. As shown in Figure 2b, the optimized Cartesian mesh discretization contains 25 squares per corner. The geometry has now a total of N = 1016 sub-regions and 46 surfaces.

2.3 Tracking parameters optimization

Here, in the same way as the previous section, the behavior of the neutronic parameters has been obtained as a function of the density d of the integration lines and the number N_a of integration angles. This study has shown that with d > 25 lines per centimeter and N_a > 25 equidistant angles in the range [0, π], the neutronic parameters remain unchanged.

To validate these two last values, we have verified the numerical integration errors made on the volumes and on the surfaces of the geometry. The number of integration angles affects only the maximum error made on the surfaces while the density of the integration lines affects both the maximum error made on the surfaces and the volumes. The central region of the geometry (the smallest circle in the central pin) limits the choice of the tracking parameters since it has the smallest volume of the geometry. By accepting errors lower than 1.0%, compared to the actual volumes and surfaces of the geometry, the optimized tracking parameters consist of N_a = 50 equidistant angles in the range [0, π] and d = 63 lines per centimeter.

3. Assembly models and simulations

3.1 Description and verification of the assembly model

As in a pressurized heavy water reactor (PHWR), the coolant flow in the SCWR core takes a loop structure. As a result, the channels configuration at the ends of the reactor core corresponds to a checkerboard pattern when we consider the coolant inflow (cold) and outflow (hot).

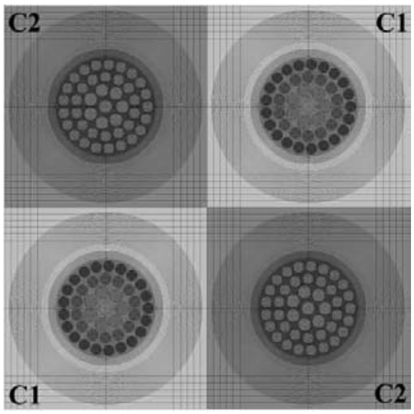

Figure 4 SCWR 2x2 assembly in checkerboard pattern

As shown in Figure 4, the 2x2 assembly in checkerboard pattern has been build from the optimized geometry (Figure 2b). It contains two different lattice cell types. The lattice cell C1 takes into account the coolant inflow and is called cooled lattice cell. The lattice cell C2 takes into account the coolant outflow and is called voided lattice cell. In this study, the coolant density of voided lattice cells is equal to 12% of the coolant density of cooled lattice cells. These conditions are those found in the SCWR under normal operation [3].

To verify the assembly model, we have first simulated the case of a 2x2 assembly containing four identical lattice cells. Isotropic reflection boundary conditions have been applied uniformly on all the external surfaces of the assembly. In this particular case, the assembly and cell calculations performed in an infinite lattice should lead to the same results.

Table 3 Comparison of k_∞ between lattice cell and 2x2 assembly of identical lattice cells

Model	**k_∞ as a function of lattice cell type**	
	Cooled lattice cell (C1)	**Voided lattice cell (C2)**
Lattice cell	1.3389	1.3451
Assembly of identical lattice cells	1.3389	1.3454

The results in Table 3 show that k_∞ increases with voiding more rapidly in the case of the assembly model than in the case of the lattice cell model. This difference is due to the effects of boundary conditions as observed in the case of the advanced CANDU reactor (ACR-700) [8]. In the lattice cell model, the isotropic boundary conditions are applied on the four external surfaces of the lattice cell. In the assembly model, the isotropic boundary conditions are only applied on the outer surfaces of the assembly leaving the inner surfaces of lattice cells with equivalent mirror like boundary conditions. It has been shown that traveling freely from one lattice cell to another in the assembly model, the neutrons increase their chances of being slowed-down by the moderator from a numerical point of view [8]. In the particular case of the voided lattice cell, this increase of neutron slowing-down leads to a significant increase of k_∞. This last point will be discussed in section 3.2.

3.2 Assembly in checkerboard pattern simulations

Now, in order to simulate an infinite checkerboard pattern, periodic boundary conditions have to be applied on all the external surfaces of the assembly of Figure 3. In our model the exact periodic boundary conditions were approximated using isotropic transmission conditions between cells (similar to isotropic reflection but for neutron transmission). From this model, the environmental effects of light water coolant density in SCWR assemblies have been studied. The k_∞ for the assembly in checkerboard pattern has been compared to the k_∞ for the cooled and voided lattice cell.

Table 4 DRAGON k_∞ for SCWR fresh fuel

	Cooled lattice cell (C1)	**Voided lattice cell (C2)**	**Assembly in checkerboard pattern**
$\mathbf{k}_\infty$	1.3389	1.3451	1.3510

From Table 4, we observed a difference of 6.2 mk between the k_∞ for the cooled and the voided lattice cell models and a difference of 5.9 mk between the k_∞ for the voided lattice cell and the assembly in checkerboard pattern models. To explain the change in k_∞ from one model to another, we must return to its definition:

$$k_\infty = \frac{\nu R_f}{R_a} \tag{1}$$

were ν is the average number of neutron produced per fission, R_f is the fission reaction rate and R_a is the neutron absorption rate. In this study, the number of neutrons produced per cell and per second, νR_f, is normalize to 1, thus:

$$k_\infty = \frac{1}{R_a} \tag{2}$$

Figure 5 presents the neutron absorption rate in the moderator region, in the coolant region and in the fuel region for the cooled and voided lattice cell as a function of the neutron energy.

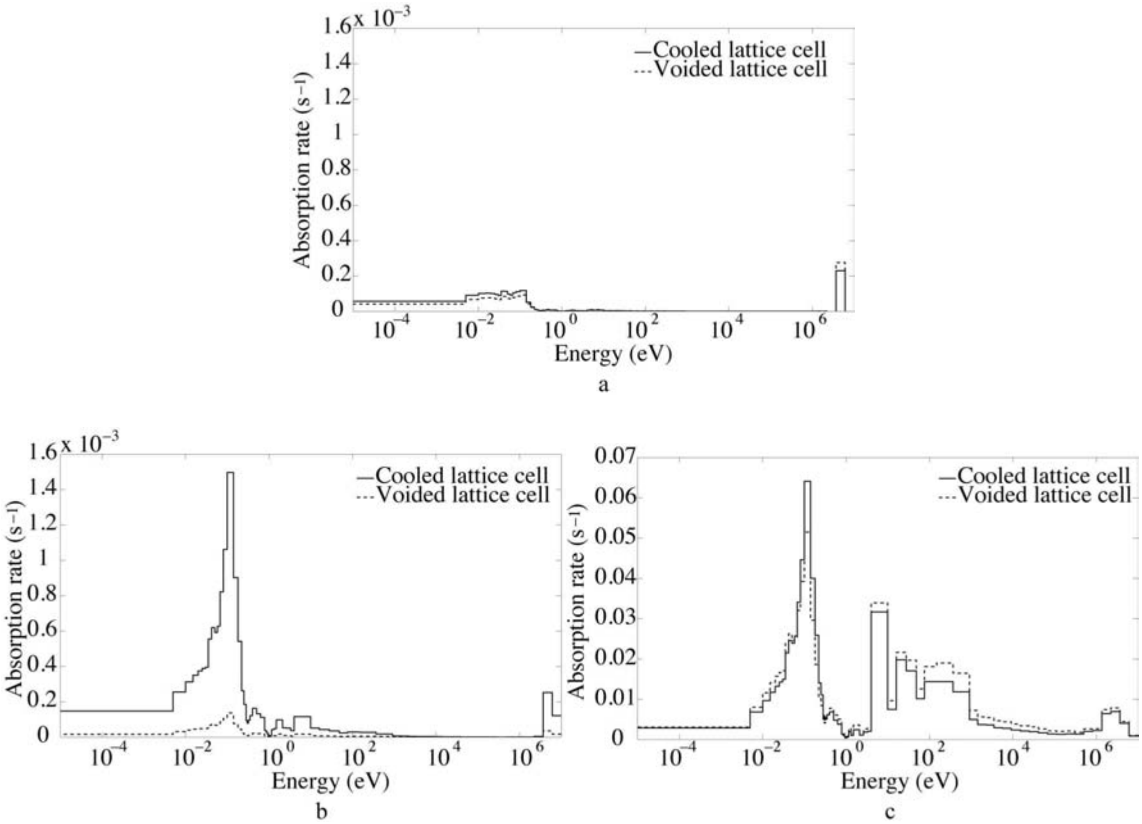

Figure 5 Neutron absorption rate in the moderator (a), coolant (b) and fuel (c) regions

The comparison of Figures 5a and 5b shows that the absorption rates in the moderator regions are much lower than those in the coolant regions. The absorption rate in the coolant region for the cooled lattice cell is about 10 times larger than the one for the voided lattice cell in the thermal energy domain ($E < 0.625$ eV). This result shows the importance of the neutron absorption in the SCWR light water coolant. This has the effect of decreasing the k_∞ for the cooled lattice cell. Figure 5c shows that the absorption rate in the fuel region for the voided lattice cell is slightly larger than the one for the cooled lattice cell in the energy domain of resonances (4 eV < E < 100 keV). This has the effect to decrease the k_∞ for the voided lattice cell, but not enough to become lower than the one for the cooled lattice cell.

Figure 6 presents the average neutron flux in the moderator, coolant and in fuel regions for the cooled and the voided lattice cell as a function of the neutron energy.

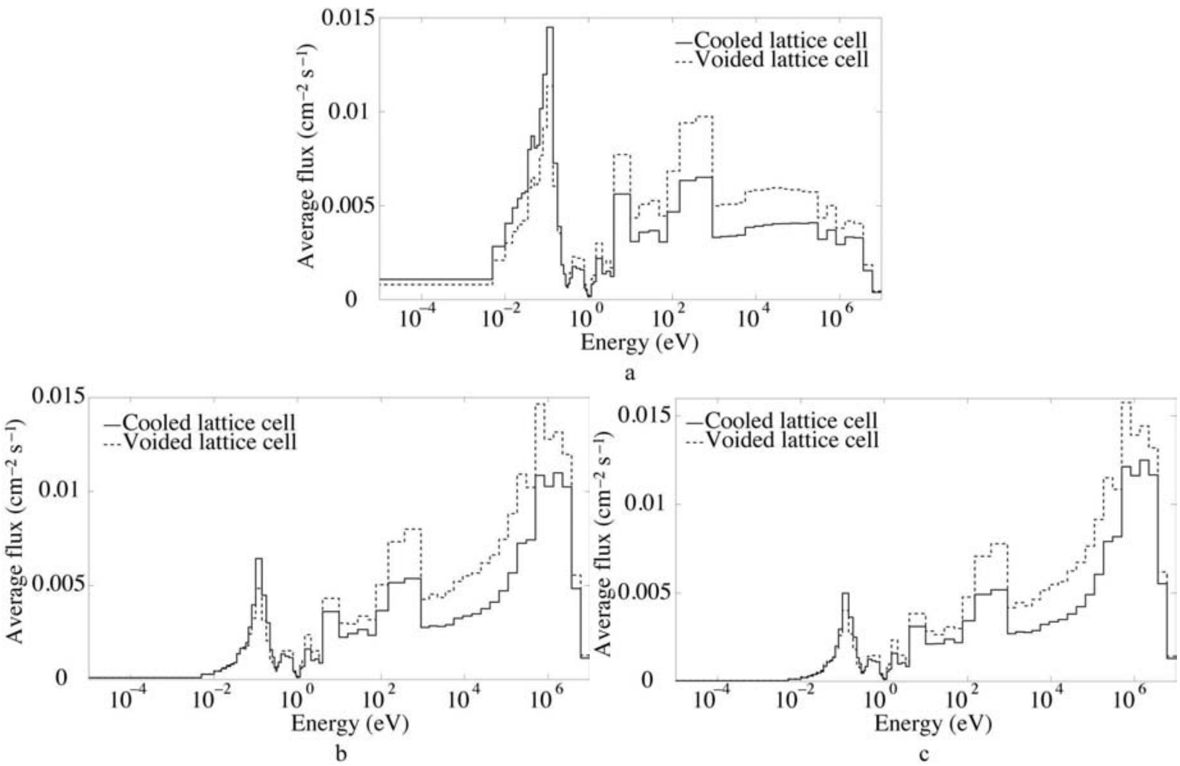

Figure 6 Average neutron flux in the moderator (a) coolant (b) and fuel (c) regions

Figure 6a shows that the average neutron flux in the moderator region for the voided lattice cell is definitely faster than the one for the cooled lattice cell. This shows the importance of the neutron slowing-down in the SCWR light water coolant. In Figures 6b and 6c one can see that the average flux in the coolant and fuel regions are similar since the fuel is immersed in the coolant. The average neutron flux in the fuel region for the voided lattice is slightly larger than the one for the cooled lattice in the energy domain of resonances. This observation explains why the absorption rate in the fuel region is more important for the voided lattice cell in this energy range.

Finally, the numerical simulations realized with the assembly in checkerboard pattern have shown that lattice cells are strongly affected by their environment. First, it must be noted that there is two times fewer cooled lattice cells in the assembly model than in the cooled lattice model. Thus, there is almost a reduction by factor of two in the neutron absorption by the coolant regions for the assembly model. This has the effect of increasing the k_∞ for the assembly.

Figure 7 presents the average neutron flux in the moderator and fuel regions and the neutron absorption rate in the fuel region for the isolated voided lattice cell and for the voided lattice cells of the assembly as a function of the neutron energy.

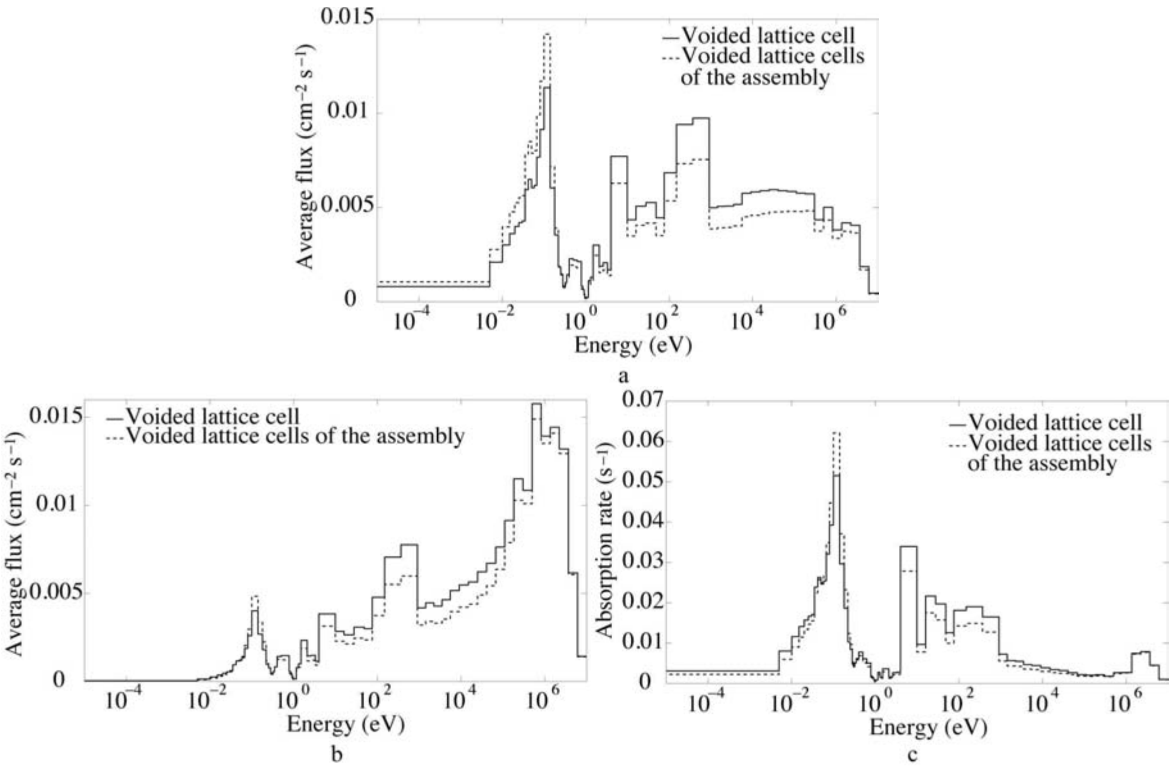

Figure 7 Average neutron flux in the moderator (a), and fuel (b) regions and the neutron absorption rate in the fuel region (c)

The comparison of the neutron spectra in Figure 7a shows that the assembly further slows-down the neutron in the moderator region for the voided lattice cells. This additional slowing-down allows more fast neutrons to escape resonance capture before reaching a second fuel element. From this fact, the assembly also reduces the average neutron flux in the fuel region in the energy domain of resonances as shown in Figure 7b. This reduction of average neutron flux results in a reduction of the neutron absorption rate in the fuel region for this energy domain as shown in figure 7c. Finally, this has the effect to increase again the k_∞ for the assembly.

4. Conclusion

In this study, the SCWR lattice cell has been modeled in the DRAGON code. Optimizations of the spatial mesh discretization and tracking parameters of the geometry are limited by the infinite multiplication constant, the product of the average number of neutron produced per fission in the thermal group and by the scattering cross section from the thermal to the fast group (group 2 to 1). This paper also presents the environmental effects of light water coolant density in SCWR models. We have demonstrated the importance of neutron absorption in light water coolant from the comparison of neutron absorption rates obtained with a cooled and a voided lattice cell. The absorption rate in the coolant region for the cooled lattice cell is about 10 times larger than that observed for the voided lattice cell in the thermal energy domain. The importance of neutron slowing-down in light water coolant from the comparison of neutron spectra is also illustrated. The average neutron flux in the moderator region for the cooled lattice cell is definitely more thermal than the one for the voided lattice cell. In the same manner, the comparisons of the results obtained from lattice cell models and assembly in checkerboard pattern have demonstrated that there is a strong coupling between neighboring cells of the SCWR. Finally, theses results show the necessity to use multicell models to optimize the safety characteristics of the Generation IV SCWR with the DRAGON and DONJON codes.

5. References

[1] U.S. DOE Nuclear Energy Research Advisory Committee and the Generation IV International Forum, ‘‘A technology roadmap for Generation IV Nuclear Energy Systems’’, *GenIV International Forum*, 2002. [On line]. Available: http://www.gen-4.org/Technology/roadmap.htm. [Consulted January 27 2009].

[2] D.F. Torgerson, B.A. Shalaby and S. Pang, ‘‘CANDU technology for generation III+ and IV reactors’’, *Nuclear Engineering and Design*, Vol. 236, 2006, pp.1565-1572.

[3] A. Abdellahi, ‘‘Étude de sûreté du SCWR par prise en compte du couplage neutronique-thermohydraulique’’, M.Sc.A., École Polytechnique de Montréal, Montréal, Québec, Canada, 2008.

[4] G. Marleau, A. Hébert and R. Roy, ‘‘A user guide for DRAGON 3.06’’, École Polytechnique de Montréal, Montréal, Québec, Canada, Technical report IGE-174 Rev. 7, 2008.

[5] E. Varin, A. Hébert, R. Roy and J. Koclas, ‘‘A user guide for DONJON’’, École Polytechnique de Montréal, Montréal, Québec, Canada, Technical report IGE-208 Rev. 4, 2005.

[6] C.K. Chow, S.J. Bushby and H.F. Khartabil, ‘‘A fuel channel design for CANDU-SCWR’’, Proceedings of the 14th International Conference on Nuclear Engineering, Miami, Florida, USA, 2006 July 17-20.

[7] E. Varin and G. Marleau, ‘‘Thermal-hydraulics instability modeling using DRAGON under supercritical pressure conditions’’, École Polytechnique de Montréal, Montréal, Québec, Canada, Technical report IGE-290, 2006.

[8] F. Talebi, G. Marleau, J. Koclas, ‘‘A model for coolant void reactivity evaluation in assemblies of CANDU cells’’, *Annals of nuclear energy*, Vol. 33, 2006, pp.975-983.